AD_____

ION MOVEMENTS IN SHOCK IN RELATION TO SURVIVAL AND ITS MODIFICATIONS

Final Report

Toshihide Sato, M.D.

January 1985

Supported by

U.S. ARMY MEDICAL RESEARCH AND DEVELOPMENT COMMAND
Fort Detrick, Frederick, Maryland 21702-5012

Contract No. DAMD17-83-C-3164

University of Maryland at Baltimore
Baltimore, Maryland 21201

DOD DISTRIBUTION STATEMENT

Approved for public release; distribution unlimited

SECURITY CLASSIFICATION OF THIS PAGE

REPORT DOCUMENTATION PAGE

Form Approved
OMB No. 0704-0188

1a. REPORT SECURITY CLASSIFICATION	1b. RESTRICTIVE MARKINGS
2a. SECURITY CLASSIFICATION AUTHORITY	3. DISTRIBUTION/AVAILABILITY OF REPORT Approved for public release; distribution unlimited
2b. DECLASSIFICATION/DOWNGRADING SCHEDULE	
4. PERFORMING ORGANIZATION REPORT NUMBER(S)	5. MONITORING ORGANIZATION REPORT NUMBER(S)
6a. NAME OF PERFORMING ORGANIZATION University of Maryland 6b. OFFICE SYMBOL (If applicable)	7a. NAME OF MONITORING ORGANIZATION
6c. ADDRESS (City, State, and ZIP Code) 10 South Pine Street Baltimore, MD 21201	7b. ADDRESS (City, State, and ZIP Code)
8a. NAME OF FUNDING/SPONSORING ORGANIZATION U.S. Army Medical Research & Development Command 8b. OFFICE SYMBOL (If applicable)	9. PROCUREMENT INSTRUMENT IDENTIFICATION NUMBER Contract No. DAMD17-83-C-3164
8c. ADDRESS (City, State, and ZIP Code) Fort Detrick Frederick, Maryland 21702-5012	10. SOURCE OF FUNDING NUMBERS PROGRAM ELEMENT NO. 61102A; PROJECT NO. 3M1-61102BS10; TASK NO. BA; WORK UNIT ACCESSION NO. 451

11. TITLE (Include Security Classification)

Ion Movements in Shock in Relation to Survival and its Modifications

12. PERSONAL AUTHOR(S)

Toshihide Sato, M.D.

13a. TYPE OF REPORT	13b. TIME COVERED	14. DATE OF REPORT (Year, Month, Day)	15. PAGE COUNT
Final	FROM 83/6/11 TO 84/12/31	1985 January	

16. SUPPLEMENTARY NOTATION

17. COSATI CODES			18. SUBJECT TERMS (Continue on reverse if necessary and identify by block number)
FIELD	GROUP	SUB-GROUP	Hemorrhagic and Bacteremic Shock, Pathophysiology, Biochemistry, Morphology, X-ray Microanalysis, RA V
06	01		
06	16		

19. ABSTRACT (Continue on reverse if necessary and identify by block number)

In order to elucidate the mechanisms of cell injury and to correlate such with ion shifts in tissues, comprehensive physiologic, biochemical, and morphological studies as well as x-ray microanalysis measurements of ions in liver and heart were performed using both in vivo hemorrhagic and bacteremic shock models in rats. In the hemorrhagic shock model, deterioration of physiologic parameters and increases in serum potassium concentrations and decreases in serum calcium concentrations were seen. In the bacteremic shock model, a hypodynamic state and increases in the activity of various enzymes released from vital organs, such as the liver or heart, were observed. Morphological results suggested that local production of free radicals from migrating and aggregated leukocytes into the sinusoids of the liver after bacteremia may play a possible role in the hepatocellular injury. In both models, x-ray microanalysis of ions in freeze-dried sections of liver and heart showed increases in sodium, chlorine and calcium and decreases in potassium and phosphorus. Data obtained as a result of these comprehensive studies not only showed a good correlation between ion shifts

20. DISTRIBUTION/AVAILABILITY OF ABSTRACT	21. ABSTRACT SECURITY CLASSIFICATION
☐ UNCLASSIFIED/UNLIMITED ☒ SAME AS RPT ☐ DTIC USERS	Unclassified
22a. NAME OF RESPONSIBLE INDIVIDUAL Mrs. Virginia Miller	22b. TELEPHONE (Include Area Code) (301) 663-7325
	22c. OFFICE SYMBOL SGRD-RMI-S

DD Form 1473, JUN 86 *Previous editions are obsolete.* SECURITY CLASSIFICATION OF THIS PAGE

FOREWORD

In conducting research using animals, the investigator(s) adhered to the "Guide for the Care and Use of Laboratory Animals," prepared by the Committee on Care and Use of Laboratory Animals of the Institute of Laboratory Animal Resources, National Research Council (NIH Publication No. 86-23, Revised 1985).

Citations of commercial organizations and trade names in this report do not constitute an official Department of the Army endorsement or approval of the products or services of these organizations.

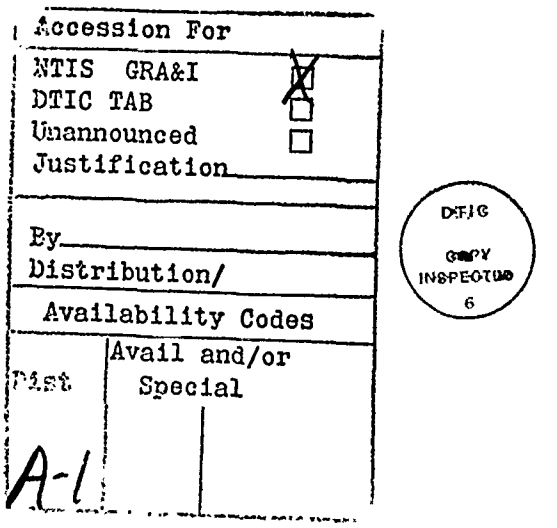

TABLE OF CONTENTS

LIST OF ILLUSTRATIONS AND TABLES

REPORT

A. PROBLEM

The understanding of the events following various types of cell injury is crucial to the development of our knowledge concerning the pathogenesis, treatment, and prevention of human diseases. Despite the advanced knowledge and treatment of hemorrhagic and bacteremic shock, mortality and morbidity continue to remain high. For better treatment of these diseases in man, much further knowledge and understanding of the cellular pathophysiology of shock is needed. It is our hypothesis that many of the cellular changes which lead the cell from normal to irreversibly injured are initiated and modified by primary and/or secondary effects of ion redistributions taking place between the cell and the extracellular compartment and between various compartments in the cell. With the recent availability of x-ray microanalysis as a tool to measure intracellular ions and thus being able to correlate structure with the chemical composition of cells, a new dimension to the analysis of cellular reactions to injury by the shock state has become possible. However, specific aspects concerning effects at the cellular and subcellular levels need to be further clarified. Therefore, the aim of this study was to characterize the cellular and subcellular effects of hemorrhagic and bacteremic shock in the liver and heart using in vivo rat models.

B. BACKGROUND

The focus of our laboratory for the past two decades has been directed toward the understanding of the events following various types of cell injury with the aim of developing knowledge which will be useful in the understanding of the pathogenesis, treatment and prevention of human diseases. Since the work of Virchow [1], the dominant concept of pathology regards disease as a result of the reactions of cells to injury. An injury can be defined as any physical or chemical stimulus which perturbs cellular homeostasis. Such a perturbation can be transient and readily adapted to by the cell with no subsequent effect or it may be a more prolonged effect to which the cell can adapt only by a series of structural and fundamental modifications or to which it succumbs, resulting in cell death. Following an injury, cell reactions can be classified into two phases: a reversible phase which precedes cell death and an irreversible phase consisting of those changes which occur after cell death. Therefore, as has now become evident, all disease states are most meaningfully expressed at the cellular and subcellular levels with such changes forming the basis of the physiologic and morphologic alterations which are observed.

Although a number of critical steps occur following injury, many of the cellular changes leading the cell from normal to irreversibly injured are initiated as well as modified by primary and secondary effects of ion redistributions. Diffusible ions such as Na, Mg, P, Cl, K, and Ca are all very important to the fine tuning of metabolic cell processes and are controlled within very narrow limits in various intracellular compartments and between the cell and the extracellular space. As a result, numerous studies over the past decade have strongly implicated an extremely important if not key role for their movements and redistributions in the pathophysiology of diverse types of cell injury such as shock, myocardial infarction, acute renal failure, metaplasia, regeneration and malignant transformation. Although all of these physiologically active ions are important, it has not been until recently that the unique role of calcium as activator and regulator of many diverse cellular activities such as contractile processes, cell division, secretory processes, enzyme activation, etc., has been realized. Since the extracellular calcium concentration is higher by several orders of magnitude than the estimated cytosolic concentration of 10^{-7} to 10^{-5} M and enters the cell by diffusion down a steep electrochemical gradient, this continuous influx of calcium implies the existence of regulatory systems for maintaining low cytosolic concentrations. Current evidence indicates that the mitochondria, plasma membrane and endoplasmic reticulum may each play a role in this control.

Although the study of ion distribution and redistributions in tissue using such methods as atomic absorption spectrophotometry, precipitation techniques, autoradiography, isotope labeling, etc. have been utilized for many years, frequently, inaccurate and misleading data have been obtained due to the difficulties associated with maintaining ion composition during the technical procedures. However, with the recent introduction of x-ray microanalysis, detailed assays of elements with atomic weights equal to Na or greater offers great promise in the study of electrolyte shifts in both normal and disease states. The technique is based on measurements of characteristic radiation resulting from interactions of electrons with matter [2] and permits, in many cases, complete non-destructive analysis by detection of characteristic x-rays which can produce information about the distribution, quantity and chemical form of an element at the cellular and subcellular levels in biological samples with a sensitivity of approximately 10^{-18} g. Areas as small as 1000 A can be measured which permit qualitative and quantitative measurements to be made on organelles and even parts of organelles. this is obviously of great value not only in studying many types of cellular inclusions but also in studying the organelle distribution of elements of physiologic importance including Na, Mg, P, Cl, K, and Ca. All of these ions have been previously impossible to localize at this level using other

techniques. Therefore, in the study of ion redistributions following cell injury, the importance of x-ray microanalysis cannot be overestimated.

Many theories have been proposed to explain the sequence of events which may lead to irreversible shock and to account for the severe changes in multiple organ systems which occur during each of these phases. Such theories have included lysosomal disruption, deficits in energy metabolism, and damage to cell membranes among others [3]. It has not been clear, however, which, if any, of these events is primary and which is secondary. In addition to the above, several studies have suggested that one important alteration involved in cell function is manifested by altered plasma membrane potential and ion shifts between extra- and intracellular compartments [3,4].

Although there have been a number of publications detailing clinical measurements by atomic absorption spectrophotometry of ion shifts following sepsis and hemorrhagic shock, to our knowledge, only the work performed in our laboratory [5,6] and that of Nichols et al. [7] has utilized the methodology of x-ray microanalysis to determine such shifts in tis-sue. Data from both of these studies were in agreement in that increases were noted in Na and Cl and decreases in K following shock.

Other investigations, using flame atomic absorption or ion specific microelectrodes, have shown leakage of K ions from cells at a relatively early stage following both septic and hemorrhagic shock [8,9]. Such leakage has been found to either precede, accompany or be followed by mitochondrial damage and cell swelling [10,11,12,13]. In order to determine if this leakage of K^+ is due to a failure in energy metabolism or to a direct effect of endotoxins on ion pumps, Kilpatrick-Smith et al. [14] investigated the effects of endotoxin in suspensions of cultured mouse neuroblastoma C-1300 cells and concluded that there were two phases of endotoxin action on these cells: the initial very rapid reaction in which mitochondrial metabolism is altered but fully compensated and the second phase in which cellular energy production by the damaged mitochondria cannot provide ATP at a sufficient rate to maintain normal cellular activities, thus leading to gradual cell death. Although the mechanism for the rapid response in energy metabolism is not clear, it could be either through a direct interaction of the endotoxin with mitochondrial membranes or enzymes or indirect through a second messenger such as intracellular Ca^{2+}. The latter is particularly intriguing to us since, if this is the case, it could link possible, subtle changes in plasma membrane permeability, which may accompany binding and transport of the toxin, and subsequent response of mitochondrial energy pr uction reactions. In accordance with this possible role of Ca^{+}, Spitzer et al. [15] and Liu et al. [16] observed that

suppressed oxidation of fatty acids by hearts of dogs which had been given endotoxin could be reversed by the addition of EDTA, therefore leading to the hypothesis that the increased level of free Ca^{2+} may have been responsible for the observed changes in metabolism. However, further experimentation is necessary to prove this point.

In direct connection with the above, and the role of ion movements in shock, it has become evident that volume regulation by cells, control of cell Na^{+} and Ca^{2+} and modulation of membranes and the cytoskeleton comprise very important if not determinate roles in a number of sublethal and lethal cell reactions to injury. Moreover, interactions of these with cell membrane modification and cytoskeletal control produce a model which, we believe, relates many important disease processes to biochemical and ultrastructural changes. Therefore, based on recent morphological, immunocytochemical and x-ray analytical data from our laboratories and those of others, we have recently advanced a hypothesis (see Appendix) which proposes that altered Na^{+} and Ca^{2+} regulation play extremely important roles in seemingly diverse pathological phenomena ranging from acute cell death to chronic processes such as shock, trauma, myocardial infarction and neoplasia and, moreover, that all of these phenomena are interrelated in a common series of cellular reactions [17,18].

It was the aim of the present study, therefore, to investigate the role of ion movements in in vivo animal models following exposure to sublethal and lethal episodes of hemorrhagic and bacteremic shock by direct analyses of intracellular ion distributions using x-ray microanalysis and to correlate these data with physiological, biochemical, and morphological observations.

C. APPROACH TO THE PROBLEM

1. Hemorrhagic Shock Model in the Rat

Male Sprague Dawley rats, weighing 250-300 g, were fasted overnight and anesthetized with phenobarbital. They were restrained in supine positions on surgical boards and allowed to breathe spontaneously without a respirator. The left carotid artery was cannulated with polyethlene tubing (PE-50) and the proximal end inserted into the aorta. Hemorrhagic shock was produced by removal of blood using suction for a period of one minute and the animals divided randomly into the following three groups:

LD 50 group = (3.16-0.18BW) ml blood/100 g body weight.
LD 84 group = (3.25-0.17BW) ml blood/100 g body weight.
Control group = cannulation only

Parameters, as described below, were measured at 0 time and 15 min after hemorrhage.

2. Bacteremic Shock Model in the Rat

Recently, we developed a bacteremic shock model in rats to study the cellular and subcellular alterations in response to lethal and sublethal Gram-negative bacteremia [19]. To establish the model, various doses of a live E. coli suspension (Serotype: O-18) were injected in conscious rats through the tail veins. Doses and mortality rates are summarized in Table 1.

Table 1. MORTALITY RATES FOLLOWING VARIOUS DOSES OF LIVE E. COLI INJECTION

Group	Dose ($\times 10^9$ Organisms/100 g BW)	Mortality Rate 6 Hrs	12 Hrs	24 Hrs
A	2.8-3.3	100% (14/14)		
B	1.8-2.0	14% (4/29)	62% (18/29)	100% (29/29)
C	1.3-1.5	0% (0/25)	8% (2/25)	96% (24/25)
D	0.4-0.5	0% (0/15)	7% (1/15)	7% (1/15)

Light microscopic studies performed on the dead animals after E. coli treatment revealed the following: 1) a dose-related depletion of white pulp in the spleen; 2) foci of small E. coli colonies in the heart only in group C in which the animals survived beyond 12 hours; 3) focal necrosis of the liver parenchyma with increased number and size of necrosis along with prolonged survival time; 4) no characteristic changes in the lung; 5) mucosal hemorrhage, vascular congestion and desquamation of the epithelium in the small intestine; and 6) medullary congestion in the kidney [19]. Groups C and D were selected as the lethal and sublethal models respectively.

On the basis of the above data, therefore, in the present contract, bacteremic shock was induced in rats by IV injection of live E. coli organisms (Sero type: O-18). E. coli organisms were inoculated in a tryptic soy broth medium from a stock culture maintained on tryptic soy agar. After stationary culture in the tryptic soy broth medium for 15 hrs at 37°C, the organisms were washed three times with sterile saline solution and resuspended in a saline solution. The number of E. coli organisms was predetermined spectrophotometrically by reading the dilute E. coli suspension at 580 nm. Twenty-four hrs later, the number of viable organisms was confirmed by colony counting. A sublethal ($0.4-0.5 \times 10^9$) or a lethal ($1.3-2.0 \times 10^9$) dose of E. coli organisms in 0.5 ml saline per 100 g body weight was injected into the tail vein with a one minute period of

injection. Saline-injected rats were used as controls. At 6, 9, 12, and 24 hrs following injection, physiological, morphologic, histochemical, biochemical and x-ray microanalysis studies were carried out as described as below.

3. Methods

The following methods were used in both the hemorrhagic and the bacteremic models.

a. Physiological Studies

An arterial catheter was introduced into the lower abdominal aorta through the left femoral artery and its external end connected to a transducer. A transpulmonary thermodilution method, which we recently developed [20], was used for the measurement of cardiac output. A thermistor probe was inserted into the right carotid artery until its tip lay in front of the aortic valve. As an indicator, 40-60 ul saline solution was injected into a central vein catheter (PE 50), which was placed close to the right atrium, through the right jugular vein. After injection of the saline, changes in blood temperature and arterial blood pressure, as well as EKGs, were simultaneously recorded on a polygraph.

b. Biochemistry

For blood chemistry determinations, the concentrations of glucose, pyruvate, lactate, creatinine, bilirubin, and the activities of S-GPT, S-OCT, CPK, LDH, and amylase were determined according to standard methods. After acid extraction from freeze-clamped livers, the concentrations of pyruvate, lactate, and adenine nucleotides were enzymatically measured.

c. Serum Electrolytes

Serum K^+ and ionized Ca^{2+} concentrations were measured by ion selective electrodes.

d. Histochemistry

Routine frozen sections were cut from liver and heart and air-dried for the determination of the following enzyme activities: AlPase, AcPase, ATPase, SDH, G6Pase, and G6PDH.

e. Morphological Studies

i) Light Microscopy

Specimens from liver and heart were fixed in a mixture of 4% formaldehyde and 1% glutaraldehyde, washed in buffer, processed through an ethanol series and embedded in paraffin. Sections of liver and heart were cut and stained with H & E.

ii) High Resolution Light Microscopy

Semi-thin sections from plastic-embedded liver and heart were prepared as described below and examined using high resolution light microscopy.

iii) Transmission Electron Microscopy

Specimens from both models were fixed as above. After post fixation with OsO_4, they were washed in buffer, dehydrated through an ethanol series and embedded in Epon 812. Ultrathin sections were cut, mounted on grids, double-stained with uranyl magnesium acetate and lead citrate and examined in a JEOL 100B electron microscope.

f. X-ray Microanalysis

Small pieces of liver and heart (0.5 mm in greatest dimension) were frozen by rapid direct immersion quenching in propane slush cooled by liquid nitrogen. Following freezing, sections 2-4 um in thickness were cut in a conventional cryostat at -20°C. While still in the cryostat, the sections were picked up onto cooled, highly polished, pure carbon planchets which were mounted on aluminum stubs. They were then transferred to a Vir-Tis Automatic Freeze-Dryer, freeze-dried under vacuum at -70°C overnight and allowed to warm slowly to room temperature the following morning. Specimens were stored in a dessicator at room temperature until examination in an AMR 1000 scanning electron microscope equipped with a LaB_6 gun, fitted with a Kevex SiLi detector and interfaced with a Tracor Northern NS 880 multichannel analyzer. Measurements were made in the scanning mode with microscope parameters as previously described. Peak to background ratios were computed using the Tracor Northern "Super ML" program according to the expression $P-B_1/B_2$ where P is the peak of interest, B_1 is the background under the peak and B_2 is the continuum between 5.50-6.50 keV after the continuum from the support film has been subtracted.

g. Statistical Analysis

In the hemorrhagic shock model, the paired two tailed Student's t test was performed to compare the pre-shock and post-shock values and Analysis of Variance was used to compare groups. In the bacteremic model, Analysis of Variance was used to determine the significant difference among groups. A value of $p < 0.05$ was considered significant.

D. RESULTS AND DISCUSSION ON THE RESULTS

1. Hemorrhagic Shock Model in the Rat

a. Physiological Studies

Detailed results of changes in CI, MABP, HR, TPR, and SVI are summarized in Table 2.

In the LD50 hemorrhagic shock group, CI decreased to 22.7% of pre-shock values at 15 min, while in the LD84 group, CI dropped to 15.1% of pre-shock values. MABP dropped to 27.8% and 23.8% of pre-shock values in LD50 and LD84 groups, respectively. TPR increased to 120% and 203% of pre-shock values in LD50 and LD84 groups, respectively. In sham-operated controls, no significant changes were noted. EKGs showed changes in the ST segment in both the LD50 and LD84 groups, indicating ischemic changes.

These data suggest that the presence of very powerful sympathetic mechanisms, induced by released cathecholamines, may, to some extent, prevent hypoperfusion in vital organs by inducing relatively well maintained HR and increased TPR.

Table 2. CHANGES IN SYSTEMIC HEMODYNAMICS FOLLOWING HEMORRHAGE

	LD50 (n=3)		LD84 (n=6)	
	0 min	15 min	0 min	15 min
CI (ml/min/kg)	312±60	71±13*	306±65	46±34*
MABP (mmHg)	141±8	39±11*	139±8	33±13*
HR (beats/min)	417±21	309±40*	416±23	303±66*
TPR (mmHg/ml/min/kg)	0.46±0.07	0.55±0.01	0.47±0.11	0.95±0.46*
SVI (ml/kg)	0.75±0.11	0.23±0.34*	0.73±0.12	0.15±0.10*

Values given are means ± S.D.; *=Significant difference ($p < 0.05$) between 0 and 15 min groups using paired t test

b. Biochemistry

Blood glucose, pyruvate, lactate, and ketone bodies were measured. Due to limited available blood after hemorrhage, fluorospectrometry for measurement of pyruvate, lactate, and ketone bodies was used. Detailed results are summarized in Table 3.

Increases in the concentrations of arterial pyruvate and lactate with decreases in the ratio of pyruvate/lactate were seen in both the LD50 and LD84 groups. However, hypoglycemia was observed only in the LD84 group.

In arterial ketone bodies, the concentration of AcAc in both the LD50 and LD84 groups decreased but that of BHOH did not significantly change, thus decreasing the ratio of AcAc/BHOH in both groups. Since the main source of production of AcAc and BHOB is the liver and since these substrates are diffusable and well regulated by the oxido-reduction state of free NAD+/NADH in liver mitochondria, the ratio of arterial AcAc/BHOB indirectly reflects the redox state of free NAD+/NADH in liver mitochondria. Despite the powerful sympathetic reflex, as indicated by the physiological monitor mentioned above, these data suggest that the oxygen supply to liver mitochondria is insufficient to produce NADH through the mitochondrial respiratory chain in both the LD50 and LD84 groups.

Table 3. CHANGES IN CONCENTRATIONS OF BLOOD GLUCOSE AND ARTERIAL PYRUVATE, LACTATE, AND KETONE BODIES FOLLOWING HEMORRHAGE

	LD50		LD84	
	0 min	15 min	0 min	15 min
Glucose	(6)109.1±14.1	109.4±20.9	(6)112.5±12.0	80.3 ±10.4*
Pyruvate	(5)0.174±0.031	0.233±0.067*	(5)0.148±0.01	0.191±0.046*
Lactate	(5) 2.57±0.63	11.29±6.39*	(5) 2.04±0.23	7.69±1.79*
$P/Lx10^2$	(5) 6.95±1.46	2.47±0.98*	(5) 7.31±0.97	2.49±0.73*
AcAc	(6)0.046±0.013	0.026±0.014*	(5)0.067±0.029	0.027±0.010*
BHOB	(6)0.170±0.116	0.171±0.113*	(5)0.165±0.107	0.152±0.067
A+B	(6)0.216±0.117	0.197±0.119	(5)0.252±0.095	0.179±0.068
A/B	(6)0.368±0.183	0.202±0.120*	(5)0.432±0.208	0.203±0.109*

Values = means±S.D.
Glucose = mg/dl
Lactate, Pyruvate, AcAc, BHOB = μmoles/ml
(n) = number of animals
* = significant difference ($p < 0.05$) between 0 and 15 min groups using paired t test

c. Serum Electrolytes

K^+ and ionized Ca^{2+} concentrations in serum were measured by ion selective electrodes. Isotonic 2, 4 and 6 mM KCl solutions for K^+ and 0.5, 1.0, and 1.5 mM $CaCl_2$ solutions for ionized Ca^{2+} were used as standards. Measurements were performed in a 25°C water bath. Results are summarized in Table 4.

Significant increases in K^+ concentrations after hemorrhage were noted, with the more severe hemorrhage inducing higher values. On the other hand, decreases in ionized Ca^{2+} concentrations in the serum after hemorrhage were observed.

Table 4. CHANGES IN K^+ AND IONIZED Ca^{2+} CONCENTRATIONS IN SERUM FOLLOWING HEMORRHAGE

		LD50			LD84	
		0 min	15 min		0 min	15 min
K^+ (mEq/L)	(8)	3.2±0.6	6.5±0.9*	(7)	3.2±0.7	6.9±1.0*
Ca^{2+} (mEq/L)	(8)	1.08±0.25	0.085±0.24*	(7)	1.06±0.36	0.82±0.31*

Values given are means±S.D.
* = significant difference ($p < 0.05$) between 0 and 15 min groups using paired t test

The availability of mini ion selective electrodes has enabled the measurement of specific ion concentrations in small amounts of serum. Since these ion selective electrodes are highly specific to certain ions and the technique is quite simple, reproducibility, therefore, is quite high [21,22,23,24].

Although the exact mechanism of hyperkalemia is unclear, x-ray microanalysis of ions in tissues, as described below, showed decreases in the concentration of K^+ in the liver and heart after hemorrhage. Thus, released K^+ from cells in their energy-depleted state may well provide the mechanism for the serum increase.

In our rat hemorrhagic shock model, the mechanism responsible for the hypocalcemia is also unclear. However, decreased oxygen supply to tissues, as mentioned above, leads to depression or depletion of cellular energy, especially ATP. This decreased cellular energy causes cessation of the Na-Ca and/or H+-Ca pumps, causing accumulation of Ca^{2+} in intracellular compartments, potentially in mitochondria and/or the endoplasmic reticulum (ER). This accumulation of Ca^{2+} in cells may cause decreased Ca^{2+} concentration in the serum. Another possible explanation is that severe hemorrhage induces cathecholamine release, as mentioned above, leading to peripheral hemostasis

which may result in intra-vascular coagulation. This requires Ca^{2+} in the serum. Thus, in addition to the accumulation of Ca^{2+} in cells, Ca^{2+} in the serum may decrease due to binding.

Harrigan et al. [25] studied changes in Ca^{2+} levels in severe shock patients during and after resuscitation. Total serum proteins, serum albumin, total Ca^{2+}, and ionized Ca^{2+} were significantly reduced. The severity of hypocalcemia paralleled the hypoproteinemia, the number of transfusions given during resuscitation, and the duration of shock. From their data, they suggested that increased extravascular Ca^{2+} flux occurs with severe shock. As mentioned above, this may, indeed, relate to the ion shifts observed in cells here in our study.

Carpenter et al. [22], in a study of hemorrhagic shock in baboons who were then resuscitated, found significant diminutions (51%) in Ca^{2+} in serum following resuscitation. Such a finding is consistent with our hypothesis in the sense of the reflow phenomenon. Reflow into previously ischemic energy depleted areas would be expected to result in an increase in intracellular Ca^{2+}, as is typically seen following reflow in ischemic myocardium. The above authors infer that such an increase in intracellular Ca^{2+} is a manifestation of the "sick cell" syndrome. This is, of course, also consistent with our own work and, indeed, emphasizes the desirability of measuring intracellular electrolytes as we have done in this study, since without measuring intracellular electrolytes, one is only dealing with an inference.

The differences in changes noted in serum Ca^{2+} during shock between our rat hemorrhagic shock model and the above-mentioned baboon model may depend upon the severity of shock, since the blood pressure in the baboons was maintained at 60 mmHg whereas the blood pressure was less than 30 mmHg in our rat model when blood samples were taken. The severe shock may cause a greater influx of Ca^{2+} into the cells, resulting in decreases in Ca^{2+} in the serum.

Carpenter et al. [22] also showed that there were changes in all forms of Mg; namely, an increase in serum Mg^{2+} during shock which then returned to normal levels after resucitation. We have not thus far observed significant changes in intracellular Mg^{2+} levels in our hemorrhagic shock model but there has been some evidence of such decreases in our bacteremic shock model as described below. These same investigators [22] also noted increases in serum phosphate levels which might well correlate with the decreased cellular phosphate levels observed in our studies as detected by x-ray microanalysis (see below).

d. X-ray Microanalysis

Typical ion measurements, using x-ray microanalysis, of 4 um freeze-dried sections of liver and heart after hemorrhage are shown in Fig. 1. 'SHAM-LIVER' and 'SHAM-HEART' represent tissues obtained from an animal in which only surgical manipulation was performed while 'EXPT-LIVER' and 'EXPT-HEART' were obtained from an animal following a 15 min interval of LD84 hemorrhagie as described in the 'Methods' section above. $P\text{-}B_1/B_2$ represents the peak (P) to background (B) ratios for each element as computed according the previously described methodology. Note the increases in Na, Cl, and Ca and the decreases in K and P in both the liver and heart from the hemorrhagic animal as compared to the sham control values. These data are in good agreement with the above serum electrolyte data since, as discussed above, a decrease in serum electrolytes corresponds to an increase in intracellular electrolytes.

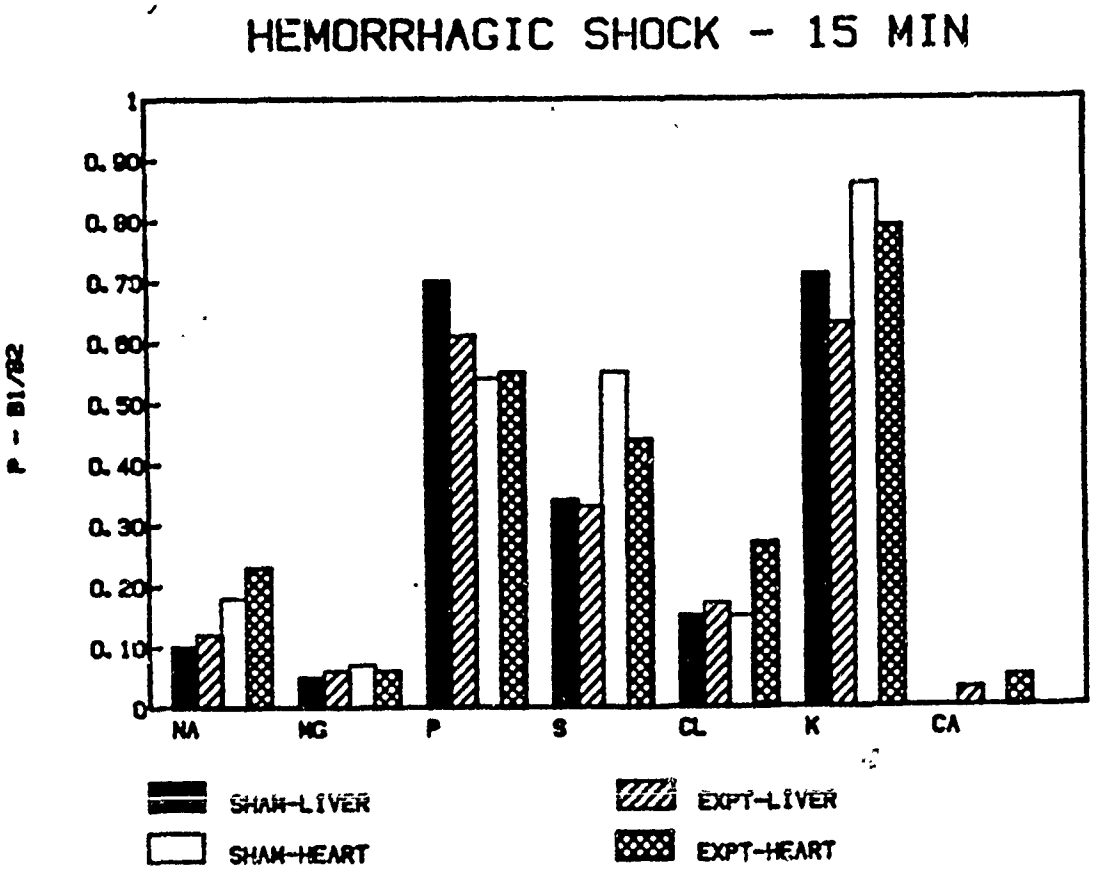

Fig. 1

2. Bacteremic Model in the Rat

i. Sublethal Bacteremia

A sublethal dose of live E. coli or saline was injected into the tail veins of conscious rats and at 6, 9, 12 and 24 hrs later, various parameters were measured.

a. Physiological Studies

The effects of sublethal E. coli bacteremia on systemic hemodynamics were studied at 6, 9, 12, and 24 hrs after the bacteremic insult. The results are summarized in Table 5. No significant changes in systemic hemodynamics were observed.

b. Biochemistry

At 6, 9, 12, and 24 hrs after sublethal bacteremia, the concentrations of blood glucose, arterial pyruvate, lactate, acetoacetate, and beta-hydroxybutyrate and serum creatinine and bilirubin as well as the activities of S-GPT, S-OCT, CPK, LDH and amylase were measured. Increases in the concentration of blood glucose were observed at 6, 9, and 12 hrs following sublethal bacteremia. However, decreases in the total ketone bodies (acetoacetate + beta-hydroxybutyrate) were noted throughout the experimental period. There were no significant changes in serum creatinine and bilirubin levels or enzyme activities. The results are summarized in Table 6.

Although as summarized in Table 7, there was no detectable deterioration of liver high energy status, decreases in the concentration of total ketone bodies (acetoacetate + beta-hydroxybutyrate) in the liver were noted, suggesting some type of metabolic change such as in carbohydrate metabolism.

Also, our recent preliminary data on citrulline production from liver homogenates (data are not shown in this report) suggest that ATP production in mitochondria following sublethal bacteremia was enhanced since the synthesis of citrulline requires ATP which is generated from intact mitochondria. This observation of a hyperfunctional mitochondrial state is in agreement with our previous work on isolated liver mitochondria following lethal bacteremia. Lethal bacteremia also induces so-called "super mitochondria" in the liver. More importantly, these changes are also induced by sublethal bacteremia and can be detected by measuring ketone body contents in the arterial blood. Changes in ketone body concentrations in the liver reflect the changes in ketone body concentrations in the arterial blood.

TABLE 5. CHANGES IN SYSTEMIC HEMODYNAMICS FOLLOWING SUBLETHAL BACTEREMIA

	6 Hrs		9 Hrs		12 Hrs		24 Hrs	
	Control (n=4)	E. coli (n=4)	Control (n=7)	E. coli (n=6)	Control (n=9)	E. coli (n=8)	Control (n=4)	E. coli (n=6)
CI	234±53	231±43	222±22	227±64	249±36	215±30	252±44.5	225±32
TPR	0.548±0.082	0.460±0.147	0.580±0.064	0.564±0.177	0.525±0.094	0.534±0.119	0.547±0.078	0.612±0.081
SVI	0.539±0.174	0.582±0.118	0.541±0.051	0.522±0.136	0.585±0.095	0.486±0.062	0.613±0.091	0.498±0.072
BP	125±12	113±11	128±10	115±18	128±11	113±14	136±21	135±5
HR	443±39	413±43	411±25	408±42	427±21	444±40	410±41	452±18

Values = mean ± SD
CI = Cardiac Index (ml/min/kg)
TPR = Total Peripheral Resistance (mmHg/ml/min/kg)
SVI = Stroke Volume Index (ml/kg)
BP = Arterial Blood Pressure (mmHg)
HR = Heart Rate (beats/min)

TABLE 6. CHANGES IN BLOOD CHEMISTRY FOLLOWING SUBLETHAL BACTEREMIA

	6 Hrs		9 Hrs		12 Hrs		24 Hrs	
	Control	E. coli	Control	E. coli	Control	E. coli	Control	E. coli
Glucose (mg/dl)	86±9.7	100±11.6	85±8.9	114±3.4	88±10.9	107±15.3	85±5.7	84±5.5
Pyruvate (nmoles/ml)	65±56.9	135±59.9	48±22.8	179±60.6	52±23.8	114±29.7	56±29.1	129±32.3
Lactate (nmoles/ml)	1485±914	2050±716	1188±386	2852±1373	1362±646	2252±548	1257±445	2194±633
P/L x 10^{-2}	4.07±1.66	6.46±1.18	4.18±1.28	6.64±1.43	4.17±1.89	5.10±0.90	4.50±1.79	5.13±1.19
AcAc (nmoles/ml)	229±63.4	94±20.4	232±41.9	113±20.8	226±47.4	102±22.8	200±34.6	101±26.0
BHOB (nmoles/ml)	703±236.4	244±64.6	768±168.0	264±89.4	807±168.9	237±43.4	542±115.8	174±39.2
A+B (nmoles/ml)	931±280.0	339±58.0	999±200.0	377±97.3	1033±169.6	339±56.7	742±143.2	275±43.7
A/B	0.356±0.132	0.412±0.151	0.309±0.049	0.460±0.136	0.294±0.099	0.436±0.098	0.377±0.053	0.610±0.209
Creatinine (mg/ml)	0.65±0.13	0.69±0.21	0.53±0.18	0.66±0.19	0.59±0.19	0.41±0.18	0.63±0.33	0.42±0.18
Total Bilirubin (mg/dl)	0.154±0.08	0.208±0.139	0.167±0.04	0.305±0.141	0.164±0.052	0.264±0.079	0.168±0.065	0.270±0.047
Direct Bilirubin (mg/dl)	0.046±0.029	0.071±0.035	0.047±0.018	0.108±0.073	0.066±0.049	0.112±0.060	0.057±0.049	0.106±0.037
GPT (U)	93±152.8	70±58.2	40±43.4	75±42.4	62±88.1	76±75.1	64±61.6	77±102.4
OCT (IU)	4.9±4.1	11.3±9.3	3.1±1.6	29±28.1	5.1±9.2	9.7±5.2	4.0±4.9	6.4±3.2
CPK (U/L)	438±362.0	538±483.1	293±154.8	621±483.6	340±142.0	408±228.3	353±250.2	334±176.6
LDH (U/L)	557±370.7	835±673.0	459±198.8	904±531.1	430±315.5	781±786.6	536±408.5	512±344.3
Amylase (SU)	1425±450	1564±565	1481±851	1058±213	1239±114	1496±688	1445±356	2072±790

Values = mean ± S.D.
(n = 6-9)

TABLE 7. CHANGES IN CONCENTRATIONS OF PYRUVATE, LACTATE, KETONE BODIES, AND ADENINE NUCLEOTIDES IN LIVER FOLLOWING SUBLETHAL BACTEREMIA

	6 Hrs		9 Hrs		12 Hrs		24 Hrs	
	Control	E. coli	Control	E. coli	Control	E. coli	Control	E. coli
Pyruvate (nmoles/g wet liver)	49±13.5	85±22.5	42±8.9	119±44.9	39±7.7	100±26.3	41±11.4	78±17.3
Lactate (nmoles/g wet liver)	757±388.0	1197±345.6	620±354.9	1346±521.6	512±254.6	1170±292.2	694±366.6	1065±474.7
P/L X 10^{-2}	8.4±5.50	7.5±1.12	8.1±3.53	9.1±2.13	9.4±4.53	8.7±1.58	6.9±2.90	8.3±4.58
AcAc (nmoles/g wet liver)	256±47.7	170±31.8	314±42.4	135±30.6	290±56.5	130±27.7	280±56.5	139±44.8
BHOB (nmoles/g wet liver)	867±255.4	415±98.8	774±165.7	319±80.2	873±223.6	329±86.0	631±52.9	328±97.8
A+B (nmoles/g wet liver)	1123±290.7	585±114.8	1087±191.0	454±68.8	1163±190.0	459±72.9	909±24.0	468±97.3
A/B	0.307±0.054	0.428±0.114	0.421±0.099	0.455±0.183	0.363±0.142	0.428±0.166	0.450±0.135	0.478±0.270
ATP (umoles/g wet liver)	2.787±0.572	2.606±0.596	2.869±0.500	2.575±0.364	2.769±0.553	2.646±0.576	2.631±0.433	2.492±0.518
ADP (umoles/g wet liver)	0.992±0.230	0.921±0.155	0.904±0.194	0.920±0.099	1.037±0.232	0.956±0.255	0.968±0.224	0.999±0.209
AMP (umoles/g wet liver)	0.238±0.060	0.234±0.064	0.217±0.052	0.202±0.053	0.210±0.046	0.229±0.068	0.237±0.073	0.233±0.068
Total (umoles/g wet liver)	4.025±0.742	3.760±0.767	3.989±0.706	3.712±0.442	4.016±0.785	3.818±0.778	3.836±0.702	3.723±0.704
Energy Charge	0.82±0.03	0.82±0.02	0.83±0.01	0.82±0.02	0.82±0.01	0.81±0.03	0.82±0.02	0.80±0.03

Values = mean ± SD
(n = 6-9)

c. Serum Electrolytes

Serum electrolyte measurements following 12 hrs of sublethal bacteremia showed a decrease in ionized Ca^{2+} and an increase in K^+ concentrations (Table 8).

Table 8. CHANGES IN K^+ AND IONIZED Ca^{2+} CONCENTRATIONS IN SERUM AT 12 HRS FOLLOWING SUBLETHAL E. COLI BACTEREMIA

	Saline	12 Hrs
K^+ (mEq/L)	3.3	3.9
Ca^{2+} (mEq/L)	2.2	1.5

ii. Lethal Bacteremia

a. Physiological Studies

The effects of lethal E. coli bacteremia on systemic hemodynamics and ICG clearance test were studied at 6, 9, and 12 hrs after a bacteremic insult. A hypodynamic state was noted at 9 and 12 hrs. The results are summarized in Table 9.

Insignificant decreases in TPR at 6 hrs was followed by significant increases at 9 and 12 hrs. This is compatible with the early hyperdynamic state seen in various experimental animals, including baboons, dogs, and rats [26,20]. The late hypodynamic state seen at 9 and 12 hrs is probably due to a combination of decreased venous return following sustained peripheral pooling and myocardial dysfunction as indicated by high CPK release in the serum (see below).

The ICG clearance test, which is a good indicator of hepatic blood flow, decreased following the bacteremic insult.

b. Biochemistry

At 6, 9, and 12 hrs after bacteremia, the concentrations of blood glucose, pyruvate, and lactate and serum creatinine and bilirubin and the activities of S-GPT, S-OCT, CPK, LDH, and amylase were measured. Hypoglycemia and lactic acidemia and increases in the concentrations of serum creatinine and bilirubin were observed. Increases in the activities of S-GPT, S-OCT and LDH and no increases in amylase were noted. The results are summarized in Table 10. As mentioned above, high CPK values were seen at 12 hrs when the hypodynamic state was well established.

Table 9. CHANGES IN SYSTEMIC HEMODYNAMICS AND ICG CLEARANCE TEST FOLLOWING LETHAL E. COLI BACTEREMIA

	Control (n=8)	6 Hrs (n=6)	9 Hrs (n=6)	12 Hrs (n=6)
CI	254±23	244±46	177±63*	182±22*
TPR	0.533±0.041	0.501±0.109	0.703±0.226*	0.679±0.086*
SVI	0.577±0.076	0.496±0.097	0.433±0.130*	0.373±0.045*
BP	135±6	114±7*	114±10*	122±21
HR	444±28	475±11	402±37*	488±25*
ICG	2.7±0.4	7.6±3.3*	8.6±4.1*	8.1±1.3*

Value = Mean±S.D.
CI = ml/min/kg
TPR = mmHg/ml/min/kg
SVI = ml/kg
MABP = mmHg
HR = beats/min
ICG = t 1/2 (min)
* = significant difference ($p < 0.05$) vs control

c. Serum Electrolytes

Concentrations of serum K^+ and Ca^{2+} were measured using ion selective electrodes. Increases in K^+ with time and initial decreases in ionized Ca^{2+} were noted. The results are shown in Table 11.

Prominent among the laboratory characteristics of staphylococcal toxic shock syndrome in patients is hypocalcemia. Recently, Chesney et al. [24] demonstrated that hypocalcemia represented a reduction in both total Ca^{2+} and ionized Ca^{2+} with elevated immunoreactive calcitonin. In experimental animals, Trunkey et al. [23] reported that the serum ionized Ca^{2+} concentration decreased during septic shock in the baboon as did the skeletal muscle extracellular pool of Ca^{2+} [27]. Using red blood cells, Shires et al. [28] demonstrated the cellular uptake of Cl^-, Na^+ and water, and a loss of K^+ during septic shock in baboons. They suggested decreased energy utilization rather than decreased energy production as a factor leading to diminished active ion transport during septic shock.

Carli et al. [29] demonstrated that septic shock sera from patients, when compared to normal sera, increased the action potential duration and depressed contractility of beating cardiac cells. Addition of Ca^{2+} reversed these two actions.

Table 10. CHANGES IN BLOOD CHEMISTRY FOLLOWING LETHAL E. COLI BACTEREMIA

	Control	6 Hrs	9 Hrs	12 Hrs
Glucose	(4) 94±14	(4) 89±15	(6) 78±12	(8) 58±21*
Pyruvate	(7)0.10±0.01	(13)0.24±0.02*	(9) 0.28±0.03*	(8) 0.23±0.01*
Lactate	(7)1.44±0.10	(13)3.35±0.33*	(9) 4.35±0.41*	(8) 4.37±0.51
Creatinine	(8)0.39±0.21	(8) 0.82±0.35*	(10)0.88±0.62*	(10)0.74±0.52*
T. Bilirubin	(9)0.15±0.04	(10)0.27±0.15	(9) 0.52±0.55*	(11)0.49±0.29*
D. Bilrubin	(8)0.04±0.01	(11)0.13±0.09*	(9) 0.22±0.37	(11)0.21±0.18*
S-GPT (U)	(7) 26±13	(9) 47±22	(6) 171±200*	(8) 173±239
S-OCT (IU)	(7) 8±5	(9) 22±14*	(10) 162±186*	(11) 207±165*
CPK (U/L)	(6) 49±27	(6) 74±38	(6) 54±12	(8) 189±91*
LDH (U/L)	(7) 74±46	(8) 540±438*	(6) 520±349*	(9) 565±483*
Amylase (SU)	(9)2683±1442	(9) 2135±495	(9) 1566±356*	(9) 1423±446*

Values = means ± S.D.
* = significant difference vs control
(n) = number of animals

Table 11. CHANGES IN K^+ AND IONIZED Ca^{2+} CONCENTRATIONS IN SERUM FOLLOWING LETHAL E. COLI BACTEREMIA

	Control	6 Hrs	9 Hrs	12 Hrs
K^+ (mEq/L)	(7) 4.0±0.8	(9) 4.7±0.8	(6) 5.0±0.5*	(8) 5.0±0.9*
Ca^{2+} (mEq/L)	(7)1.70±0.14	(7) 1.24±0.32*	(6) 1.40±0.20	(8) 1.36±0.50

Values = means±S.D.
* = significant difference vs control
(n) = number of animals

Again, as mentioned above, all of these results are compatible not only with our serum electrolyte data but also with our x-ray microanalysis data since a decrease in serum electrolytes corresponds to an increase in intracellular tissue electrolytes.

d. Histochemistry

After lethal bacteremia, AlPase, AcPase, ATPase, SDH, G6Pase and G6PDH were performed on liver frozen sections. Increases in AlPase activity, due to the positive activity over the leukocytes which had migrated into the sinusoid, and increases in AcPase activity in the parenchymal cell were noted. The increases in AcPase activity in the parenchymal cells indicated the quantitative increases in the number of secondary lysosomes. ATPase, SDH, G6Pase, and G6PDH showed no significant changes.

e. Morphological Studies

Routine light microscopic observations showed infiltration of leukocytes surrounding foci of bacterial colony in the heart during hypodynamic state after E. coli bacteremia. Recently, Manson and Hess [30] hypothesized that oxygen free radicals from leukocytes contribute to the characteristic myocardial dysfunction of endotoxin shock. Free radicals can directly affect the function and activity of the excitation-contraction coupling system of cardiac muscle.

Plastic-embedded semi-thin sections of liver were examined using high resolution light microscopy. Foci of hepatocellular injury were observed as increasing in size and number with time. Focal accumulation of fibrin and degeneration and debris of leukocytes in the sinusoids were observed. Focal accumulation of lipid droplets with time was also noted.

Electron microscopy showed swollen mitochondria and increases in the number of autophagic vacuoles with time. The increased number of autophagic vacuoles observed in the hepatocytes of these animals is of great interest. In previous studies, we have characterized and analyzed this phenomenon in various models including that in which autophagy is induced by infusion by glucagon or administration of vinblastine [31,32]. We also have been observing massive increases in the number of autophagic vacuoles in tissues from biopsies and/or immediate autopsies of patients with severe sepsis in our trauma unit [33]. . This phenomenon appears to be related to modification of the cytoskeleton, perhaps occasioned by intracellular messengers including Ca^{2+}. This might explain the induction of this phenomenon by glucagon as well as vinblastine. In <u>in vitro</u> studies in our laboratory have been successful in reproducing autophagy using the Ca ionophore A23187, which increases Ca

influx [34]. The increased number of autophagic vacuoles, noted in the present study, also correlated with the light microscopic demonstration of increased activity of acid phosphatase, a well-known lysosomal marker. Such increased autophagy is one of the principle known means of organelle turnover and may correlate with the increased protein catabolism observed in animals and patients with sepsis.

The mitochondrial swelling observed in the hepatocytes is also of interest and represents an early, although reversible, change following a variety of types of cell injury. It is our hypothesis that this swelling directly correlates with modification of intracellular electrolytes. An increase of ionized Ca^{2+} in the cytosol could activate phospholipases which modify mitochondrial inner membrane permeability.

The mechanism of damage to the hepatocytes in bacteremia and/or sepsis, of course, is an important question. In our bacteremic model, these lesions were predominantly seen in the areas where leukocytes had migrated and aggregated, suggesting that there is some correlation between the infiltration of leukocytes and the damage to hepatic parenchymal cells. One possible mechanism, as shown in our working hypothesis [17,18], is membrane damage from complement, endotoxins, or toxic products of leukocytes such as superoxide and related metabolites.

f. X-ray Microanalysis

Typical ion measurements, using x-ray microanalysis, of 4 um freeze-dried sections of liver and heart after bacteremia are shown in Fig. 2. 'SALINE C - LIVER' and 'SALINE C - HEART' represent tissues obtained from an animal in which saline only was injected into the tail vein while '9 HR-BACT-LIVER' and '9 HR-BACT-HEART' were obtained from an animal 9 hrs following an injection of a lethal dose of E. coli organisms. $P\text{-}B_1/B_2$ represents peak (P) to background (B) ratios for each element as computed according to previously described methodology. Note the increases in Na, Cl, and Ca and the decrease in P in both the liver and heart following the bacteremic episode as compared to the saline-injected controls. Note also that K decreases in the liver but increases in the heart. Such an increase in K has been noted by Clemens et al. [35] in hepatocytes following sepsis in micropuncture areas of hyperpolarization. Again, as mentioned above, x-ray microanalysis of intracellular ions adds considerably to our knowledge of changes occurring in bacteremia by indicating clearly that such shifts or redistributions do, indeed, occur.

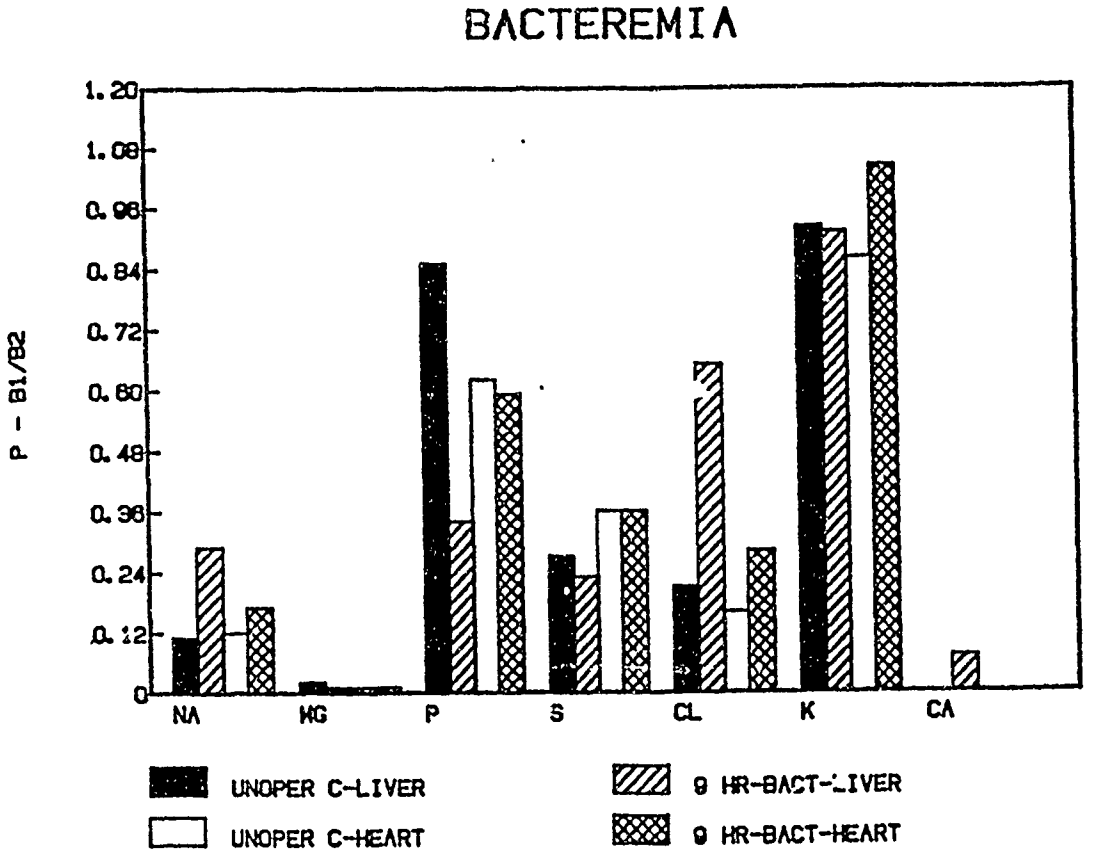

Fig. 2

E. CONCLUSIONS

In our in vivo rat hemorrhagic shock model, measurements of intracellular ion shifts, as determined by x-ray microanalysis of freeze-dried 4 um sections of liver and heart, correlated with the significant changes seen in serum K^+ and ionized Ca^{2+} concentrations as well as with the physiologic, biochemical, and morphological parameters described above. The depressed energy production, due to the decreased oxygen delivery, resulted in inhibition of the active membrane transport, causing the intracellular ion shifts. These intracellular ion shifts may well provide the mechanism for the increase in K^+ and the decrease in the ionized Ca^{2+} concentration in the serum.

In addition, x-ray microanalysis measurements revealed decreases in phosphorus. Although serum phosphate levels were not measured in our study, Carpenter et al. [22] have shown that they did increase significantly during hemorrhagic shock in the

baboon. The above would, therefore, agree with the hypothesis that a decrease in serum electrolyte levels corresponds to increases in intracellular ion levels.

The bacteremia rat model closely approximates the pathophysiology and subcellular changes seen in patients with sepsis. It is striking that the morphological changes in the heart and liver correspond so closely with observations made in this laboratory on tissues from traumatized humans with sepsis from our Immediate Autopsy Program [33]. The subcellular changes in the liver in those studies consisted of focal mitochondrial swelling and a large increase in the number of autophagic vacuoles and secondary lysosomes. Focal accumulation of leukocytes and fibrin as well as degeneration and debris of the leukocytes in the sinusoids and focal lipid accumulation in hepatocytes were also often observed in the rat model in the present studies.

Mitochondrial swelling correlated with increased Na^+, decreased K^+, and increased Ca^{2+} in the hepatocytes. In previous work on simplified models *in vitro* [36], these phenomena occurred simultaneously. In our hypothesis, this is not fortuitous but may be causally interrelated. The increased Na^+, in some cells at least, leads to Ca^{2+} efflux from the mitochondria and, at the same time, to an increase in intracellular Ca^{2+}, possibly through decresed Na-Ca exchange. Although at the present time, there is question regarding this mechanism in the liver, it is clear that increases in Ca^{2+} result in uncoupling of mitochondrial oxidative phosphorylation and mitochondrial swelling. No precipitates of Ca^{2+} in the form of hydroxyapatite occurred in the liver mitochondria in the bacteremic shock model, in contrast to other types of cell injury as noted in our Flowchart (see Appendix).

The autophagic vacuoles seen in the hepatocytes of the bactermic model were not only striking but also represented a striking parallel with changes seen in the human shock liver. Autophagic vacuoles, not commonly known in medicine, may represent an important sublethal reaction to injury. When these form, there is a budding of the cytosolic contents into the lumens of the cytocavitary network. In our hypothesis [17,18], this represents a form of cytosolic blebbing, in this case, into the endoplasmic reticulum cisternae rather than into the extracellular space.

Finally, it is important to recognize that the changes seen in the liver vary from area to area. Indeed, in histologic sections, the changes are regional, involving local degeneration and local accumulation of leukocytes and fibrin in the sinusoids. Among the advantages of x-ray microanalysis is the possibility of evaluating differences in ion shifts in different

cells and to correlate these with changes in subcellular systems, other intracellular events, and other changes such as accumulation of leukocytes. It is our working hypothesis that one mechanism of cell injury is from membrane damage. The toxic products of infiltrated leukocytes such as superoxide and related metabolites may play a possible role in such regional cell injury.

F. RECOMMENDATION

The studies conducted during this contract period have clearly validated the utility of these two *in vivo* models for the study of hemorrhagic and bacteremic shock, respectively. The results with the bacteremic model have been particularly exciting and, therefore based on the results and observations described in this report, it is logical that we extend our studies with the following goals:

1. to characterize ion shifts in more detail at the organelle level, using x-ray microanalysis, in livers and hearts from our *in vivo* bacteremic shock animal model and to correlate such with physiological, biochemical, and morphological data;

2. to explore the role of oxygen free radicals released from infiltrated leukocytes on hepatocellular injury and cardiac dysfunction seen in the hypodynamic state;

3. to explore the nature of protein catabolism as indicated by our observation of increased autophagic vacuoles and secondary lysosomes;

4. to explore the effects of various interventions such as

   a. non-steroidal anti-inflammatory agents and cortico-steroids which alter production of oxygen free radicals as well as membrane stability, and;

   b. calcium entry blockers which modify intracellular ion shifts;

5. to study ion shifts in tissues from the in vivo model, using x-ray microanalysis, following various interventions and to correlate such with physiological, biochemical, and morphological data.

In future studies, in vitro rat hepatocyte and myocyte models could be used and the same biochemical and morphological techniques as described above performed, including x-ray microanalysis of intracellular ions. Comparison of responses of the rat hepatocyte model with a human hepatocyte model could be included in future studies.

LITERATURE CITED

1. Virchow, R.: Vorlesungen uber Pathologie, Berlin, Hirschwald, 1863.

2. Chandler, J.A.: X-ray microanalysis in the electron microscope. In: Practical Methods in Electron Microscopy. Vol. 6 (Glauert, A.M., ed.), North-Holland Publ. Co., Amsterdam, pp. 317-547, 1977.

3. Baue, A.E.: Multiple, progressiver or sequential system failure. A syndrome of the 1970's. Arch. Surg. 110:779-781, 1975.

4. Trump, B.F.: The role of cellular membrane systems in shock. In: The Cell in Shock, The Upjohn Co., Kalamazoo, MI., pp. 16-29, 1974.

5. Trump, B.F., Berezesky, I.K., Chang, S.H., Pendergrass, R.E., and Mergner, W.J.: The role of ion shifts in cell injury. Scanning Electr. Microsc. 3:1-13, 1979.

6. Trump, B.F., Laiho, K.U., and Berezesky, I.K.: The role of ion movements in cell injury and shock. Circ. Shock 6:182, 1979.

7. Nichols, B.L., Bilbrey, G.L., Hazelwood, C.F., Kimzey, S.L., Liu, C.T., Viteri, F., Alvarado, J., and Beisel, W.R.: Sequential changes in body composition during infection; Electron probe study. IV. Amer. J. Clin. Nutr. 30:1439-1446, 1977.

8. Cunningham, J.N., Shires, G.T., and Wagner, Y.: Cellular transport defects in hemorrhagic shock. Surgery 70:215-222, 1971.

9. Silver, I.A.: Ion movements induced by endotoxin in cultured cells. Circ. Shock 5:221-222, 1978.

10. DePalma, R.G., Harano, Y., Robinson, A.V., and Holden, W.D.: Structure and function of hepatic mitochondria in hemorrhage and endotoxemia. Surg. Forum 21:3-6, 1970.

11. DePalma, R.G., Levy, S., and Holden, W.D.: Ultrastructure and oxidative phosphorylation of liver mitochondria in experimental hemorrhagic shock. J. Trauma 10:122-132, 1970.

12. Schumer, W., Erve, P.R., and Obernolte, R.P.: Endotoxemic effect on cardiac and skeletal muscle mitochondria. Surg. Gynecol. Obstet. 133:433-436, 1970.

13. Schumer, W., Gupta, T.K.D., Moss, G.S., and Nhyus, L.M.: Effect of endotoxemia on liver cell mitochondria in man. Ann. Surg. 171:875-882, 1970.

14. Kilpatrick-Smith, L., Erecinska, M., and Silver, I.A.: Early cellular responses in vitro to endotoxin administration. Circ. Shock 8:585-600, 1981.

15. Spitzer, J.J., Bechtel, A.A., Archer, L.T., Black, M.R., and Hinshaw, L.B.: Myocardial substrate utilization in dogs following endotoxin administration. Amer. J. Physiol. 227:132-136, 1974.

16. Liu, M.S., and Spitzer, J.J.: In vitro effects of E. coli endotoxin on fatty acid and lactate oxidation in canine myocardium. Circ. Shock 4:181-190, 1977.

17. Trump, B.F., Berezesky, I.K., and Phelps, P.C.: Sodium and calcium regulation and the role of the cytoskeleton in the pathogenesis of disease: A review and hypothesis. Scanning Electr. Microsc. 2:434-454, 1981.

18. Trump, B.F. and Berezesky, I.K.: The role of sodium and calcium regulation in toxic cell injury. In: Drug Metabolism and Drug Toxicity (Mitchell, J.R., and Horning, M.G., eds.), Raven Press, New York, pp. 261-300, 1984.

19. Tanaka, J., Sato, T., Jones, R.T., Trump, B.F., and Cowley, RA: The pathophysiology of septic shock: Responses to different doses of live Escherichia coli injection in rats. Adv. Shock Res. 9:101-114, 1983.

20. Sato, T., Isoyama, T., Tanaka, J., Jones, R.T., Cowley, R A., and Trump, B.F.: The pathophysiology of septic shock: Changes in hemodynamics in rats following live E. coli injection. An application of the thermodilution method for measurement of cardiac output. Adv. Shock Res. 7:25-42, 1982.

21. Moore, E.W.: Ionized calcium in normal serum, ultrafiltrates, and whole blood determined by ion-exchange electrodes. J. Clin. Invest. 49:318-334, 1970.

22. Carpenter, M.A., Trunkey, D.D., and Holcroft, J.: Ionized calcium and magnesium in the baboon: Hemorrhagic shock and resuscitation. Circ. Shock 5:163-172, 1978.

23. Trunkey, D., Carpenter, M.A., and Holcroft, J.: Ionized calcium and magnesium: The effect of septic shock in the baboon. J. Trauma 18:166-172, 1978.

24. Chesney, R.W., McCarron, D.M., Haddad, J.G., Hawker, C.D., DiBella, F.P., Chesney, P.J., and Davis, J.P.: Pathogenic mechanisms of the hypocalcemia of the staphylococcal toxic-shock syndrome. J. Lab. Clin. Med. 101:576-585, 1983.

25. Harrigan, C., Lucas, C.E., and Ledgerwood, A.M.: Significance of hypocalcemia following hypovolemic shock. J. Trauma 23:488-493, 1983.

26. Hinshaw, L.B., Brackett, D.J., Archer, L.T., Beller, B.K., and Wilson, M.F.: Detection of the "hyperdynamic state" of sepsis in the baboon during lethal E. coli infusion. J. Trauma 23:361-365, 1983.

27. Holcroft, J.W., Trunkey, D.D., and Carpenter, M.A.: Extracellular calcium pool decreases during deep septic shock in the baboon. Ann. Surg. 192:683-686, 1980.

28. Shires, G.T., III, Peitzman, A.B., Illner, H., and Shires, G.T.: Changes in red blood cell transmembrane potential, electrolytes, and energy content in septic shock. J. Trauma 23:769-774, 1983.

29. Carli, A., Auclair, M.-C., Vernimmen, C., and Jourdon, P.: Reversal by calcium of rat heart cell dysfunction induced by human sera in septic shock. Circ. Shock 6:147-157, 1979.

30. Manson, N.H., and Hess, H.L.: Interaction of oxygen free radicals and cardiac sarcoplasmic reticulum: Proposed role in the pathogenesis of endotoxin shock. Circ. Shock 10:205-213, 1983.

31. Arstila, A.U., Shelburne, J.D., and Trump, B.F.: Studies on cellular autophagocytosis: A histochemical study on sequential alterations of mitochondria in the glucagon-induced autophagic vacuoles of rat liver. Lab. Invest. 27:317, 1972.

32. Hirsimaki, P., Trump, B.F., and Arstila, A.U.: Studies on vinblastine-induced autophagocytosis in the mouse liver. I. The relation of lysosomal changes to general injurious effects. Virchows Arch. Cell Pathol. 22:89, 1976.

33. Champion, H.R., Jones, R.T., Trump, B.F., Decker, R., Wilson, S., Miginski, M., and Gill, W.: A clinico-pathologic study of hepatic dysfunction following shock. Surg. Gynecol. Obset. 142:657, 1976.

34. Jokinen, I., Hirsimaki, Y., and Arstila, A.U.: Autophagocytosis induced by ionophore A23187 and low calcium medium in EATC. J. Ultrastructr. Res. 69:149, 1979.

35. Clemens, M.G., Chaudry, I.H., and Baue, A.E.: Hepatic membrane potentials in early and late sepsis. Circ. Shock 10:245, 1983.

36. Laiho, K.U., and Trump, B.F.: Mitochondrial changes, ion and water shifts in the cellular injury of Ehrlich ascites tumor cells. Beitr. Pathol. Bd. 155:237-247, 1975.

GLOSSARY

AcAc = acetoacetate
A+B = acetoacetate + beta-hydroxybutyrate
A/B = acetoacetate/beta-hydroxybutyrate
AcPase = acid phosphatase
AlPase = alkaline phosphatase
ATPase = adenosine triphosphatase
BHOB = beta-hydroxybutyrate
Ca = calcium
Ca++ = ionized calcium
CI = cardiac index (ml/min/kg)
CPK = creatine phosphokinase
Creatinine = mg/dl
D. Bilirubin = direct bilirubin (mg/dl)
Energy Charge = (ATP + 1/2 ADP)/(ATP + ADP + AMP)
ER = endoplasmic reticulum
Glucose = mg/dl
GPT = alanine aminotransferase
G6Pase = glucose-6-phosphatase
G6PDH = glucose-6-phosphatase dehydrogenase
HR = heart rate
Lactate = nmoles/ml
LDH = lactate dehydrogenase
MABP = mean arterial blood pressure
Mg++ = ionized magnesium
OCT = ornithine carbamoyltransferase
Pyruvate = nmoles/ml
P/L = pyruvate/lactate
SDH = succinate dehydrogenase
SVI = stroke volume index
TPR = total peripheral resistance
T. Bilirubin = total bilirubin (mg/dl)

APPENDIX

A. FLOWCHART ILLUSTRATING OUR HYPOTHESIS OF THE RELATIONSHIPS AMONG Na^+ AND Ca^{2+} REGULATION, THE CYTOSKELETON AND THE CELLULAR REACTIONS WHICH ENSUE.

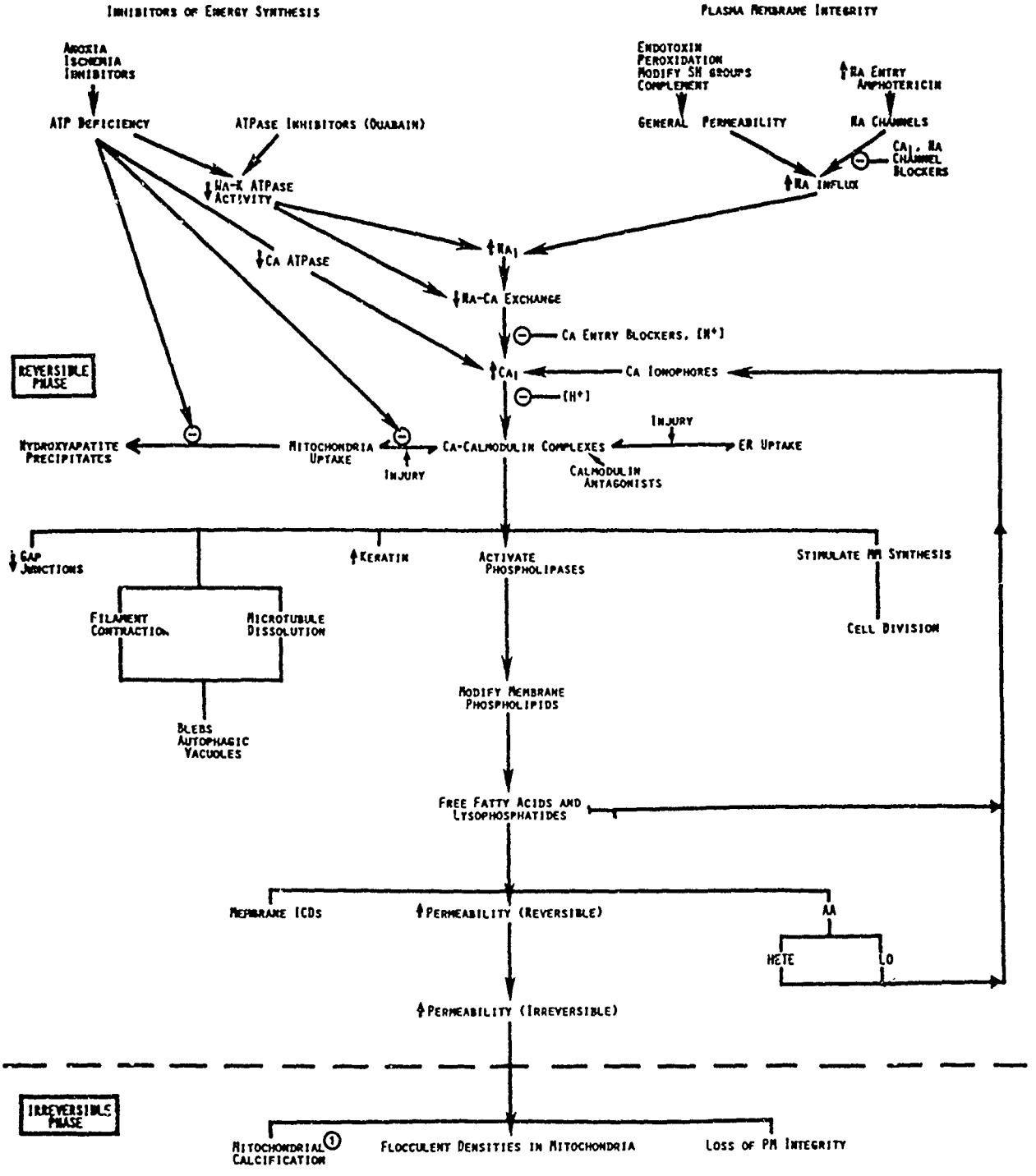

① ONLY IF MITOCHONDRIAL FUNCTION IS NOT INHIBITED

(From Trump, B.F. and Berezesky, I.K.: Role of sodium and calcium regulation in toxic cell injury. IN: Drug Metabolism and Drug Toxicity, Chapter 13, Mitchell, J.R. and Horning, M.G., eds, Raven Press, New York, pp. 261-300, 1984.)

B. LIST OF PUBLICATIONS SUPPORTED BY THIS CONTRACT.

Berezesky, I.K., Sato, T., Hirai, F., Nakatani, T., and Trump, B.F.: The role of ion shifts in a rat hemorrhagic shock model. Fed. Proc. 43:326, 1984.

Berezesky, I.K., Sato, T., Nakatani, T., Hirai, F., and Trump, b.F.: Intracellular ion movements in an in vivo bacteremic shock animal model. Circ. Shock 13:100, 1984.

Sato, T., Berezesky, I.K., Hirai, F., Nakatani, T., and Trump, B.F.: Ultrastructural changes in migrating leukocytes in the liver following lethal E. coli bacteremia in rats. Proc. Electr. Microsc. Soc. Amer. pp. 182-183, 1984.

240

THE EFFECTS OF SPLENECTOMY ON AN EXPERIMENTAL RAT INTRA-ABDOMINAL ABSCESS MODEL. T. Sato*, T. Nakatani*, F. Hirai*, and B.P. Trump. University of Maryland School of Medicine, Department of Pathology, Baltimore, MD 21201.

Recently, we developed a highly reproducible intra-abdominal abscess model in the rat by inoculation of a rat fecal pellet with or without 10^7 E. coli into the abdominal cavity which produced 100% abscess formation at the abscess stage (Fed Proc 42:1251, 1983). In the present experiments, the effects of splenectomy on this model were studied. Splenectomy was performed simultaneously with inoculation of the fecal pellet in young Sprague-Dawley rats. Splenectomy induced a higher mortality rate at the peritonitis stage (by 48 hrs after inoculation of the pellet) as also did the lower doses of E. coli (10^3). Continuous body weight loss was observed in half of the rats with splenectomy and E. coli during the abscess stage. An E. coli abscess with or without splenectomy resulted in a hyperdynamic state, high cardiac output and low peripheral resistance. The hepatic energy status deteriorated with the abscess. Splenectomy alone or splenectomy with a sterile fecal pellet induced no death and no body weight loss during the abscess stages. These data suggest that the spleen plays a key role in systemic resistance and that splenectomy may change the stable abscess stage to an unstable abscess stage. (Supported in part by NIH Grant #1R01 GM32084.)

241

THE ROLE OF ION SHIFTS IN A RAT HEMORRHAGIC SHOCK MODEL. I.K. Berezesky*, T. Sato*, F. Hirai*, T. Nakatani*, and B.F. Trump. University of Maryland School of Medicine, Department of Pathology, Baltimore, MD 21201.

Extra- and intracellular ion shifts may play a key role in cell injury. To correlate ion shifts and cell injury using physiologic and biochemical parameters, LD84 or LD50 hemorrhagic shock rats were produced by withdrawing a precalculated volume of blood within a one minute period and parameters monitored before and at 15 minutes after hemorrhage. Cardiac output was proportional to the severity of hemorrhage and EKGs showed ischemic changes. After hemorrhage, hypoglycemia and lactic acidosis were noted but no significant increases in LDH and OCT release in serum were observed. Serum electrolyte concentrations, as measured by ion selective electrodes, showed increases in potassium and decreases in calcium after hemorrhage. X-ray microanalysis of ions in freeze-dried sections of heart and liver showed increases in sodium and chlorine and decreases in potassium concentrations. These data not only show good correlation between ion shifts and hemorrhagic shock as monitored by physiologic, biochemical and x-ray microanalytical parameters but also that ion shifts do play an important if not determinant role in cell injury. (Supported by Army Contract #DAMD17-83-C-3164.)

242

EFFECT OF ENDOTOXIN ON BLOOD GASES & pH IN CONSCIOUS RATS. W. Law*, P. Donahue*, M. Brottman*, P. Gama Filho*, R. Davis,* & J. Ferguson. U of IL at Chicago H.S.C., Chicago, IL 60680.

Rats are used extensively in models of endotoxin shock. However, little is known about the effects of endotoxin on blood gases in rats. In this study male, Sprague-Dawley rats, weighing 300-400 gm, were anesthetized with 2 ml/kg Equi-Thesin (Jen-Sal Co.) i.p. for cannulation of blood vessels (right carotid artery and jugular vein) with PE-50 polyethylene tubing (Fisher Sci. Co.). 24 hours after surgery, each conscious rat received endotoxin (6 or 10 mg/kg i.v.; E. coli lipopolysaccharide; Difco). Blood gases were measured on a Corning 168 blood gas/pH analyzer. Total hemoglobin (Hb) was measured according to the method of Henry. Results from arterial samples are presented in the table below.

Dose	Time**	pH	PCO_2	PO_2	HCO_3	TCO_2	Hb
6 mg /kg	0	7.44	37.8	90.6	25.6	26.7	14.8
	10	7.41	33.9	96.7*	21.8	22.8*	16.3
	30	7.38	28.7*	103.6*	17.1*	17.9*	15.8
	60	7.39	23.4*	108.4*	14.2*	14.9*	13.3
10 mg /kg	0	7.49	36.4	87.6	27.7	28.8	----
	10	7.46	24.1*	96.7	17.9*	18.6*	----
	30	7.41	12.9*	117.9*	8.4*	8.8*	----
	60	7.03	18.7*	120.9*	5.2*	5.8*	----

*$p < 0.01$ by LSD after anova **min. post-endotoxin.

These results indicate that endotoxin can cause dramatic dose related changes in arterial blood gases in rats that are unrelated to pH. Supported by Lola Wilson Grant #48309.

243

RELATIONSHIP OF STRUCTURE AND FUNCTION FOR THE U.S. REFERENCE STANDARD ENDOTOXIN EXPOSED TO ^{60}CO-RADIATION. Gyorgy Csako, Eva A. Suba, Alice Ahlgren, Chao-Ming Tsai and Ronald J. Elin. National Institutes of Health, Federal Drug Administration and Naval Medical Research Institute, Bethesda, MD.

The relationship between the structure and function of bacterial endotoxins is poorly understood. We used ionizing radiation from a ^{60}Co-source to physically detoxify the highly purified bacterial endotoxin, the U.S. Reference Standard Endotoxin (RSE). Alterations in the structure of the RSE were assessed with the electron microscope and by electrophoresis. The biological function of the irradiated RSE was assessed with the limulus amebocyte lysate test, mouse lethality, anticomplementary activity for guinea pig complement, local Shwartzman reaction in rabbits, mitogenicity for mouse spleen cells and platelet aggregation using dog platelets. The results show a direct relationship between the degradation of the molecular and supra-molecular structure and loss of biological function. However, there was variability among the functional assays in their rate of change with progressive irradiation of the RSE. These studies suggest that it may be possible to selectively alter the endotoxin molecule to preserve positive factors for the host while eliminating toxicity.

BIOMEDICAL ENGINEERING I (244–245)

244

PULSE DUPLICATOR APPARATUS FOR SIMULATING VASCULAR HEMODYNAMICS IN VITRO. Harvey S. Borovetz, Arthur M. Brant*, Eva M. Sevick*, E. Christis Farrell*, Edwin C. Klein*, and Conrad Wall*. Dept. of Surgery, University of Pittsburgh, Pgh., Pa.

A pulse duplicator apparatus (PDA) has been developed for simulation in vitro of vascular hemodynamics. The PDA is characterized by the realistic pulsatile flow of radiolabelled (^{14}C-4) serum cholesterol through excised canine carotids. A unique feature of its design is that such variables as mean pressure, transmural pressure, pulse pressure, heart rate, and arterial flow rate may be independently varied, and the hemodynamic response of the carotid artery to these flow processes studied in detail. Sixteen perfusion studies, each of two hour duration, have been conducted to date using freshly excised canine carotids in the PDA. The hemodynamic simulation corresponded to the normal vascular case with pulse frequency = 1/sec, T=37°C, mean flow rate ~ 150 cc/min, and the pressure waveform ~120 mm Hg/80 mm Hg (mean 100 mm Hg). Among the interesting findings from these experiments are: 1) the overall uptake of ^{14}C-4 cholesterol by the artery is not controlled by boundary layer phenomena; 2) the distribution of radiolabelled serum within the various layers of the wall of the artery shows a steep gradient within the intima/media which reduces to zero in the adventitial region; 3) the waveform for the instantaneous radial dilation lags that for proximal pressure by ~10°. The peak instantaneous flow rate lags the maximal dilation of the vessel by ~45°.

245

MODEL BASED STUDY OF THE CLOSED-LOOP BAROREFLEX CONTROL OF TOTAL PERIPHERAL RESISTANCE IN THE CAT. Roberto Burattini, Piet Borgdorff# (Dept. of Electronics & Automatica, Univ. of Ancona, Italy. Lab. for Physiol., Free Univ., Amsterdam, The Netherlands)

We quantified the steady-state baroreflex regulation of total peripheral resistance in closed-loop condition. In eight lightly anesthetized cats we varied cardiac output by graded caval vein occlusion. The static relationship between mean arteriovenous pressure gradient and mean flow, which was convex to the pressure axis, was described by a model. The model consists of a nonlinear negative-feedback control system where control pressure was assumed as reference pressure. The ratio of the steady-state change in peripheral resistance to the change in arterial pressure (resistance gain, G_R) is a constant parameter in the model. We used an automatic identification procedure to estimate G_R from the experimental pressure-flow data. The estimates varied, in the different animals, from 0.002 to 0.010 min/ml. When the baroreflex sensitivity was diminished by deepening anesthesia, G_R decreased by 35 to 50% and could become zero with very deep anesthesia. We then linearized our model about the control operating point and computed the overall open-loop gain G_O. The values of G_O varied from 0.64 to 2.30 during light anesthesia and decreased by the same percen-

Circ. Shock 1984 13:100

These studies demonstrate that irreversible injury to ATP generating mechanisms occurs during hypoxia. Loss of AMP may play a role. Cellular inorganic phosphate levels may be a more sensitive indicator of oxygen-deprivation injury than ATP. The mechanism of this injury is independent of intracellular acidosis.

140

REVERSE TRIIODOTHYRONINE EXACERBATES MORTALITY AFTER SMAO SHOCK. S. HALEVY, M. LIU-BARNETT, B.M. ALTURA. Dept. of Anesthesiology, SUNY at Stony Brook, NY 11554 and Dept. of Physiology, SUNY Downstate Medical Center, Brooklyn, NY 11203.

Reverse triiodothyronine (rT3) is an ubiquitous thyroid hormone found in large concentrations in the blood of patients and experimental animals with a variety of acute or chronic non-thyroidal illnesses. Although the cardiovascular actions of the thyroid hormones, T3 and T4 are well-known, the precise effects, if any, that rT3 exerts on the cardiovascular system have not been described. During some of our experiments, we noticed that an increase in serum rT3 seemed to parallel the severity of vascular changes and mortality after shock. In view of the latter and the paucity of data on rT3, we initiated experiments on rats subjected to superior mesenteric arterial occlusion (SMAO) shock. The immediate and long-term effects of a single administration of 3,3,5-triiodothyronine (rT3) on survival and plasma T3 and T4 was studied in male Wistar rats. Thyroid hormone levels were assessed by radioimmunoassay. Mortality was found to increase by 160 percent in rT3-treated animals. Plasma T3 and T4 levels decreased in control animals treated with rT3. However, rT3-treated animals exhibited significantly lower T3 and T4 than controls or untreated animals when subjected to SMAO for 20 min. These results suggest that rT3 may play an important role in the pathophysiology of circulatory shock.

141

INTRACELLULAR ION MOVEMENTS IN AN IN VIVO BACTEREMIC SHOCK ANIMAL MODEL. I.K. BEREZESKY*, T. SATO*, T. NAKATANI*, F. HIRAI*, B.F. TRUMP*. (Introduced by: R.T. Jones). Department of Pathology, University of Maryland School of Medicine, Baltimore, MD 21201.

In order to elucidate the mechanisms of cell injury following bacteremic shock in an in vivo rat model, intracellular ion shifts were measured in serum using ion selective electrodes and in unfixed, freeze-dried cryosections of liver and heart using x-ray microanalysis (XRMA). Bacteremic shock was induced by IV injection into the tail vein of a lethal dose ($1.3\text{-}2.0 \times 10^9$) of live E. coli organisms. Saline-injected rats were used as controls. At 6, 9, and 12 hrs following the bacteremic insult, serum K^+ and Ca^{2+} levels were measured. For XRMA, small pieces of liver and heart were rapidly quench-frozen, cryosectioned, freeze-dried and analyzed. Serum electrolyte measurements showed increases in K^+ and initial decreases in Ca^{2+} with time as compared to controls. XRMA revealed increases in Na, Cl and Ca and decreases in K, P, and Mg in both organs following bacteremia. These data are consonant with each other in that decreases in serum electrolytes correspond to increases in intracellular ions. However, even more importantly, the excellent correlation of these data with our physiological, biochemical, and morphological results illustrates the extrapolation of ion shifts as measured by x-ray microanalysis to the structural and functional manifestations of bacteremia. As to the mechanisms involved, the results are compatible with our hypothesis that deregulation of ions, particularly Ca^{2+}, triggers a variety of events involving the cell membrane and the cytoskeleton which lead to irreversible injury and thus cell death. (Supported by Army Contract No. DAMD17-83-C-3164 and NIH GM32084.)

142

PROTECTION AGAINST SALMONELLA TYPHIMURIUM BACTEREMIA IN RODENTS BY IMMUNOGLOBULIN THERAPY. M.S. COLLINS*, J.M. LURTON*, M.M. EVERETT*, T.E. EMERSON, JR. Cutter Group of Miles Labs, Berkeley, CA 94710

Mortality during bacteremia shock remains high despite treatment with specific antibodies and other agents. This study was undertaken to determine the efficacy of a recently developed "native" 5% IgG preparation for i.v. use (IGIV) against severe bacteremia.

G. W. Bailey, Ed., *Proceedings of the 42nd Annual Meeting of the Electron Microscopy Society of America*

ULTRASTRUCTURAL CHANGES IN MIGRATING LEUKOCYTES IN THE LIVER FOLLOWING LETHAL E. COLI BACTEREMIA IN RATS

T. Sato, I.K. Berezesky, F. Hirai, T. Nakatani and B.F. Trump

University of Maryland School of Medicine, Department of Pathology, Baltimore, MD 21201

Hepatocellular injury and dysfunction after Gram-negative sepsis have been well recognized in both humans and experimental animal models (1,2) with circulating septic components being attributed to producing the hepatocellular injury. We have previously shown, in a lethal E. coli bacteremic rat model, the progressive migration of leukocytes and foci of hepatic lesions along with release of liver enzymes (2). In those studies, hepatic lesions were randomly scattered throughout the liver but were prominent in midzonal regions where migrated and aggregated leukocytes were frequently seen, suggesting that there may be some correlation between the presence of leukocytes and damage to hepatic parenchymal cells (2). In the same model, infiltration of leukocytes into the myocardial interstitium was also noted (3), possibly contributing to the observed myocardial dysfunction.

In the present study, ultrastructural changes in migrating leukocytes in liver following lethal E. coli bacteremia in rats were studied. Adult male rats were fasted for 15 hrs. A lethal dose of live E. coli (Serotype: O-18; 1.3 to 2.0 x 10^9 organisms per 100 gm of body weight) was injected in conscious rats through the tail vein within a 1 min period. Saline-injected rats were used as controls. Animals were sacrificed at 3, 6, and 12 hrs after injection. Livers were fixed, processed and ultrathin sections examined with a JEOL 100B electron microscope.

After bacteremic treatment, progressive migration of leukocytes and fibrinoid deposits in sinusoids were apparent with time. Migrating leukocytes with dense cytoplasm frequently contained engulfed E. coli organisms (Fig. 1). With digestion of organisms, the leukocyte cytoplasm became enlarged and less dense and contained heterosomes and vacuoles (Fig. 2). Some of the leukocytes contained numerous heterosomes or secondary lysosomes with degeneration of cytoplasmic organelles (Fig. 3). Frequently, degenerated leukocytes, with a "watery" cytoplasm and containing vacuoles and secondary lysosomes, were phagocytosed by Kuppfer cells (Fig. 4). These degenerated leukocytes in the sinusoids increased in number with time. Hepatocellular damage, such as dilatation of the ER and swelling of mitochondria along with increased numbers of phagocytosomes or secondary lysosomes, also increased with time.

Knowledge of the possible mechanisms involved in bacteremia or sepsis which cause hepatocellular injury and dysfunction needs much further investigation. In addition to altered microcirculation and circulating septic components such as endotoxins produced by bacteremia or sepsis, one possible mechanism may be membrane damage from the toxic products of the migrating leukocytes such as oxygen free radicals and related metabolites. These oxygen free radicals have been shown to cause extensive cellular damage in several tissues following endotoxemia including endothelial cell damage, phospholipid membrane lysis, damaged mitochondria, lysosomal disruption and increased vascular permeability (4). Acid hydrolases released during the digestion of these microorganisms and from the degenerated leukocytes in the sinusoids may also be involved. Thus, the regional production of oxygen free radicals and related metabolites as well as acid hydrolases may play a key role in the hepatocellular injury and dysfunction seen in bacteremia or sepsis. (Supported by NIH GM32084 and Army Contract DAMD 17-83C-3164).

REFERENCES

1. H.R. Champion et al. Surg. Gynecol. Obstet. 142(1976)657.
2. T. Sato et al. Lab. Inv. 47(1982)304.
3. J. Tanaka et al. Adv. Shock Res. 9(1983)101.
4. N.H. Manson and H.L. Hess. Circ. Shock 10(1983)205.

Fig. 1. Leukocytic migration containing engulfed E. coli (E).
Fig. 2. Leukocytes containing numerous secondary lysosomes (arrows).
Fig. 3. Degenerated leukocyte.
Fig. 4. Degenerated leukocyte undergoing phagocytosis by Kuppfer cell (K).

C. PERSONNEL WHO RECEIVED CONTRACT SUPPORT.

S. Kawashima, M.D.

I.K. Berezesky, B.A.